Supporting Material

S1. Detection selectivity for the two differently labeled lysozyme solutions.

The intensity diagrams in Figures S1.1 and S1.2 show the selectivity in the detection of the two differently labeled lysozyme solutions. No instrumental setting was changed between the scannings of Figures S1.1 and S1.2.

(a) (b)

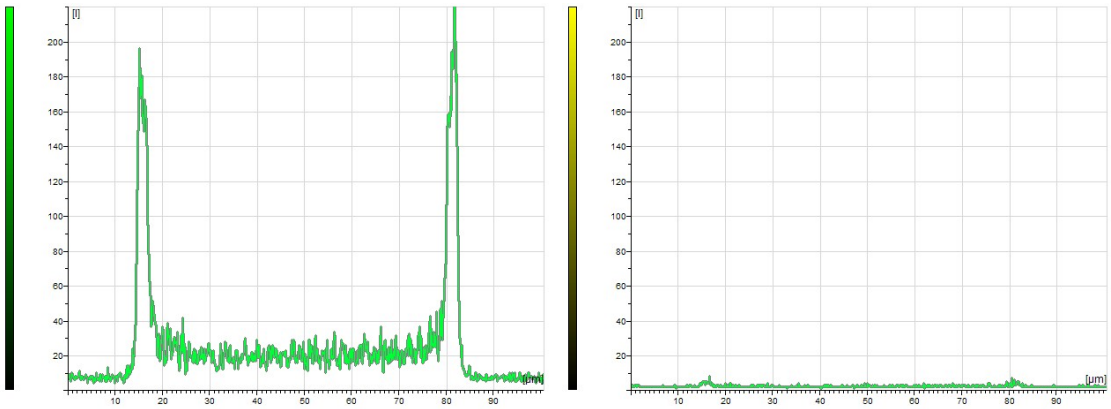

Figure S1.1. Emission intensity diagrams, representing a "cut" through the centre of a microgel particle, after uptake of Oregon Green 488-labeled lysozyme. Emission intensities are registered at (a) 500-530 nm after excitation with 488 nm, and at (b) 650-750 nm after excitation with 633 nm.

(a) (b)

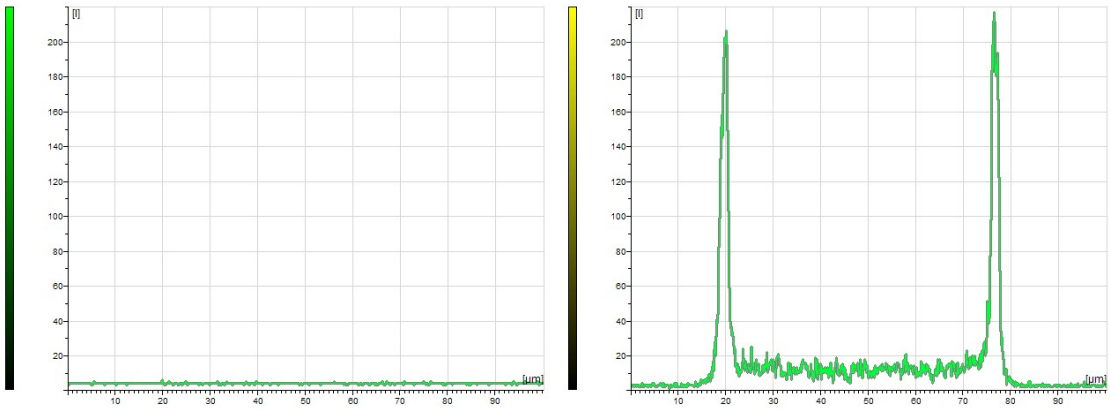

Figure S1.2. Emission intensity diagrams, representing the centre layer of a microgel particle, after uptake of Alexa Fluor 647-labeled lysozyme. Emission intensities are registered at (a) 500-530 nm after excitation with 488 nm, and at (b) 650-750 nm after excitation with 633 nm.

S2. Derivation of kinetic equations

For a protein with net charge Z we define an overall protein-to-polymer charge ratio in the gel:

$$\beta = \frac{n_{pr} Z}{n_{pol}} \qquad \text{(S:1)}$$

and a corresponding ratio for the protein in the shell:

$$\beta_{shell} = \frac{n_{pr}^{shell} Z}{n_{pol}} \qquad \text{(S:2)}$$

where n_{pr} and n_{pr}^{shell} is the number of moles of protein molecules in the whole gel and in the shell, respectively, and n_{pol} the number of moles of polymer charged groups in the gel. Note, β and β_{shell} include only stationary protein molecules.

The volume of the gel in osmotic equilibrium with the solution prior to protein binding can be written:

$$V_0 = \frac{4\pi R_0^3}{3} = n_{pol} v_0 \qquad \text{(S:3)}$$

where R_0 is the initial gel radius, and v_0 is the volume per mole of polymer charged groups in the gel prior to protein binding. To find a relationship between the gel volume V and the number of bound protein molecules we let f_{shell} denote the local polymer-to-protein charge ratio in the shell, so that the fraction of polymer located in the shell is $f_{shell}\beta_{shell}$. If the volume of the shell per mole of polymer charged groups in it is equal to v_{shell} the total shell volume equals $n_{pol}f_{shell}\beta_{shell}v_{shell}$. Thus, the volume of the core is $n_{pol}(1\text{-}f_{shell}\beta_{shell})v_{core}$, where v_{core} is the volume per mole of polymer charge, assumed constant throughout the entire core. Since the total gel volume is the sum of the shell and core volumes we obtain:

$$\frac{V}{V_0} = \left(\frac{r_2}{R_0}\right)^3 = f_{shell}\beta_{shell}\frac{v_{shell}}{v_0} + \left(1 - f_{shell}\beta_{shell}\right)\frac{v_{core}}{v_0} \qquad \text{(S:4)}$$

where the last term on the r.h.s. is the core volume V_{core} normalized by V_0:

$$\frac{V_{core}}{V_0} = \left(\frac{r_1}{R_0}\right)^3 = \left(1 - f_{shell}\beta_{shell}\right)\frac{v_{core}}{v_0} \qquad \text{(S:5)}$$

By letting f_{cdl} represent the local polymer-to-protein charge ratio in the core diffusion layer, we obtain in a similar way for the protein free part of the core:

$$\left(\frac{r_0}{R_0}\right)^3 = \left(1 - f_{shell}\beta_{shell} - f_{cdl}(\beta - \beta_{shell})\right)\frac{v_{core}}{v_0} \qquad \text{(S:6)}$$

The steady state transport rate of protein through the core diffusion layer and the shell are given by eqs. (S:7) and (S:8), respectively [1, 2]:

$$\frac{dn_{pr}}{dt} = \frac{4\pi r_0 r_1 D_{cdl}\left(C_1^{cdl} - C_0^{cdl}\right)}{r_1 - r_0} \qquad \text{(S:7)}$$

$$\frac{dn_{pr}}{dt} = \frac{4\pi r_1 r_2 D_{shell}\left(C_2^{shell} - C_1^{shell}\right)}{r_2 - r_1} \qquad \text{(S:8)}$$

In these expressions, D_{cdl} is the diffusion constant of the mobile protein in *cdl* and D_{shell} is the value in the shell. C_a^{cdl} and C_a^{shell} are the concentrations of mobile protein in *cdl* and the shell respectively at r_a. Mass transfer from the bulk solution to the gel surface can be described by the Sherwood number (*Sh*) [3]. At steady state this can be written [4]:

$$\frac{dn_{pr}}{dt} = 4\pi r_2\left(1 + Sh/2\right)D\left(C_{bulk} - C_2^{liq}\right) \qquad \text{(S:9)}$$

where C_{bulk} and C_2^{liq} is the concentration of it in the bulk liquid and in the liquid at r_2, respectively, and D is the diffusion constant of the protein in the liquid.

The requirement of local equilibrium provides relationships between the protein concentration on each side of the boundaries at r_1 and r_2:

$$C_2^{shell} = k_{shell/liq} C_2^{liq} \tag{S:10}$$

$$C_1^{shell} = k_{shell/cdl} C_1^{cdl} \tag{S:11}$$

where $k_{\alpha/\beta}$ is the partition coefficient for the distribution of protein between regions α and β (see Supporting Material S3). Since, at steady state, the transport rate must be the same in all regions, eqs. (S:7) - (S:11) can be combined to give:

$$\frac{dn_{pr}}{dt} = \frac{4\pi R_0^3}{3Zv_0}\frac{d\beta}{dt} = \frac{4\pi P_{shell}\left(C_{bulk} - C_0\right)}{\left\{r_1^{-1} - r_2^{-1} + \left(r_0^{-1} - r_1^{-1}\right)P_{shell}/P_{cdl} + r_2^{-1}P_{shell}/D'\right\}} \tag{S:12}$$

where

$$D' = (1 + Sh/2)D \tag{S:13}$$

$$P_{shell} = D_{shell} k_{shell/liq} \tag{S:14}$$

$$P_{cdl} = D_{cdl} k_{cdl/liq} \tag{S:15}$$

Finally, it follows from the assumption that the protein transport is rate determining that r_0, r_1, and r_2 can be considered as functions of β only. Therefore eq. (S:12) can be integrated to give:

$$t = \frac{R_0^3}{3v_0 Z(C_{bulk} - C_0)} \int_0^{\beta} \left\{ \left(r_0^{-1} - r_1^{-1} \right) P_{cdl}^{-1} + \left(r_1^{-1} - r_2^{-1} \right) P_{shell}^{-1} + r_2^{-1} D'^{-1} \right\} d\beta \qquad \text{(S:16)}$$

Eq. (S:16) is quite general for steady-state transport in the geometry in Figure 1b. When applied to the theory outlined above one uses eqs. (S:4) – (S:6) to substitute for $r_0 - r_2$. The equation can then be used to calculate the time for a gel to reach a certain β value, which in turn provides the corresponding values of $r_0 - r_2$.

S3. Partition coefficients.

At pH 7 the liquid solution contains mainly lysozyme (L^{Z+}), Na^+ (M^+), and $H_2PO_4^-$ (A^-). The chemical potentials for the electrolytes LA_Z and MA can be written:

$$\mu_{LA_Z} = \mu_{L^{Z+}}^0 + RT \ln C_{L^{Z+}}^{liq} + Z\mu_{A^-}^0 + ZRT \ln C_{A^-}^{liq} \qquad \text{(S:17)}$$

$$\mu_{MA} = \mu_{M^+}^0 + RT \ln C_{M^+}^{liq} + \mu_{A^-}^0 + RT \ln C_{A^-}^{liq} \qquad \text{(S:18)}$$

where "0" denotes the standard state. Local equilibrium at r_2 requires that the chemical potential of both electrolytes are the same in the shell and the liquid solution. In as much as the form of eq. (S:17) and (S:18) is valid for the mobile electrolytes in the shell, the equilibrium conditions can be written:

$$C_{L^{Z+}}^{shell} \left(C_{A^-}^{shell} \right)^Z = C_{L^{Z+}}^{liq} \left(C_{A^-}^{liq} \right)^Z = C_{L^{Z+}}^{liq} C_{salt}^Z \qquad \text{(S:19)}$$

$$C_{M^+}^{shell} C_{A^-}^{shell} = C_{M^+}^{liq} C_{A^-}^{liq} = C_{salt}^2 \qquad \text{(S:20)}$$

where we have noted that $C_{A^-}^{liq} = C_{M^+}^{liq} = C_{salt}$. The electroneutrality condition for the shell can be written:

$$ZC_{L^{Z+}}^{shell} + f_{shell}^{-1} v_{shell}^{-1} + C_{M^+}^{shell} = v_{shell}^{-1} + C_{A^-}^{shell} \qquad \text{(S:21)}$$

Eqs. (S:19-21) represent a system of equations from which $C_{L^{Z+}}^{shell}$, $C_{A^-}^{shell}$, and $C_{M^+}^{shell}$ can be calculated from v_{shell}, f_{shell}, C_{salt}, and $C_{L^{Z+}}^{liq}$ using an iterative procedure. If $ZC_{L^{Z+}}^{shell} << f_{shell}^{-1} v_{shell}^{-1}$, the first term in eq. (S:21) can be neglected, and one obtains:

$$k_{shell/liq} = \frac{C_{L^{Z+}}^{shell}}{C_{L^{Z+}}^{liq}} = \left(\frac{C_{salt}}{C_{A^-}^{shell}} \right)^Z \approx \left(\frac{C_{salt}}{Z\left(f_{shell}^{-1} - 1\right) v_{shell}^{-1} / 2 + \left(\left(Z\left(f_{shell}^{-1} - 1\right) v_{shell}^{-1} / 2 \right)^2 + C_{salt}^2 \right)^{\frac{1}{2}}} \right)^Z \qquad \text{(S:22)}$$

Eq. (S:22) is a good approximation when the protein concentration in the liquid in contact with the gel is low and when f_{shell} does not deviate too much from unity.

Local equilibrium at r_1 can be handled in a similar way, but requires in the general case additional relationships provided by eqs. (S:7) - (S:9) and the steady-state condition. However, in the limit of low mobile protein concentrations on both sides of the phase boundary we have:

$$k_{shell/cdl} = \frac{k_{shell/liq}}{k_{cdl/liq}} \qquad \text{(S:23)}$$

where $k_{cdl/liq}$ is given by eq. (S:22) with "*shell*" replaced "*cdl*".

The neglect of activity coefficients in the above expressions is reasonable as long as there is excess salt in both phases, and the concentrations of the mobile and stationary protein are low. Note also that the concentration of stationary proteins are unaffected by variations in the mobile protein concentration (i.e., the aggregated structure is considered to be "saturated" with protein).

S4. Model fitting in the absence of stagnant layer; $(D')^{-1}=0$.

By substituting for $r_0 - r_2$ using eqs. (S:4) – (S:6), putting $v_{core}= v_0$, and applying the conditions eqs. (5a,b), the integral in eq. (1; S:16) can be calculated analytically. The result can be expressed as the time to reach a state during shell formation (t_{shell}):

$$t_{shell} = \frac{R_0^3}{3v_0 Z C_{bulk} P_{shell} f_{shell}} \left\{ 1 - \left(f_{shell}\beta_{shell}\right)^{\frac{2}{3}} + \frac{\left(1+\left(v_{shell}/v_0 - 1\right)f_{shell}\beta_{shell}\right)^{\frac{2}{3}} - 1}{v_{shell}/v_0 - 1} \right\} \qquad \text{(S:24)}$$

and during core diffusion (t_{core}):

$$t_{core} = t_{shell} + \frac{R_0^2\left(I_1 + I_2\right)}{2v_0 Z C_{bulk} P_{core} f_{cdl}} \qquad \text{(S:25a)}$$

where

$$I_1 = \left(1 - f_{shell}\beta_{shell,\infty}\right)^{\frac{2}{3}} - \left(1 + \left(f_{cdl} - f_{shell}\right)\beta_{shell,\infty} - f_{cdl}\beta\right)^{\frac{2}{3}} \qquad \text{(S:25b)}$$

is the contribution to t_{core} from the diffusion through *cdl*, and

$$I_2 = \left(\left(P_{shell}^{-1} - P_{core}^{-1} \right) \left(1 - f_{shell} \beta_{shell,\infty} \right)^{-\frac{1}{3}} - P_{shell}^{-1} \left(1 - f_{shell} \beta_{shell,\infty} \left(1 - v_{shell} / v_0 \right) \right)^{-\frac{1}{3}} \right) \left(\beta - \beta_{shell,\infty} \right) \quad \text{(S:25c)}$$

is the contribution from the diffusion through the shell.

To fit eq. (S:24) to experimental data of r_2 as a function of t, one can eliminate β_{shell} from the expression using:

$$\beta_{shell} = \frac{\left(r_2 / R_0 \right)^3 - 1}{f_{shell} \left(v_{shell} / v_0 - 1 \right)} \quad \text{(S:26)}$$

obtained from eq. (S:4). Since P_{shell} is a function of f_{shell} through eqs. (S:19) – (S:21) and eq. (S:14), this leaves f_{shell} as the only adjustable parameter.

In cases where t_{shell} is easy to determine directly from the experimental curves, eq. (S:24) offers a short cut to determinations of f_{shell}.

S5. Calculation of R_0 and v_0

Figure S5.1 shows the volume v_0 per polymer charge of microgels in protein-free solutions plotted as a function of *log* of the salt concentration [5]. A least-square fit resulted in the following relationship:

$$v_0 = 0.0223 + 0.00741 \times \log\left(C_{salt} / mM \right) \quad \text{(S:27)}$$

All gels in the present study had a radius of 35±5 μm in a reference 220 mM salt solution, where according to eq. (S:27) v_0=0.0051 m^3/mol. The radius R_0 at lower ionic strengths is therefore given by:

$$R_0 = \left(\frac{v_0}{0.0051\, m^3 / mol} \right)^{\frac{1}{3}} \times 35 \mu m \qquad \text{(S:28)}$$

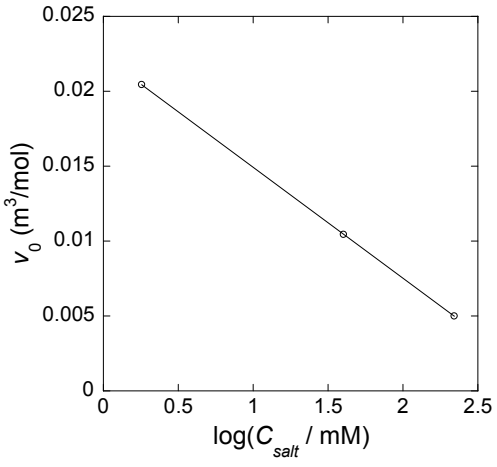

Figure S5.1. The volume v_0 per polymer charge of microgels in protein-free solutions plotted as a function of *log* of the salt concentration in the liquid. Data taken from previous work [5].

S6. Dependence of model fitting parameters on δ_∞

As noted above, the fits were obtained for a final shell thickness δ_∞ equal to 5 μm, a value determined for the 0.25 g/L sample in the confocal microscopy study. The fact that the variation of δ_∞ did not change much as the protein concentration in the solution increased from 0.25 to 1 g/L gives some credit to using the same value also at lower concentrations, but the differences in the conditions during protein binding in the two experiments introduces uncertainties. The limited resolution of the light microscope prevented accurate measurements of the shell thickness, but as a rough estimate δ_∞ was found to be 5 ± 2 μm. To test how the uncertainty in δ_∞ influences on the determination of the parameters, we repeated the fitting procedure for a number of different δ_∞. The result is presented in Figures S6.1 and S6.2. It was found that the model fitted nearly equally well in a wide range, and so there is no unique set of parameters giving the best fit. (Outside the range set by the curves in Figs. S6.1 and

S6.2 the model could not be fitted to the data). However, common to all experimental conditions is that f_{shell} is quite insensitive to both δ_∞ and protein concentration in the solution, and never deviates much from unity. Some of the other parameters showed a strong variation with δ_∞, in particularly the stationary and mobile protein concentration in the shell. Importantly, however, for any variation of δ_∞ within the estimated range (5 ± 2 μm), it is clear that ϕ_{shell} is larger at 100 than at 40 mM salt. Furthermore, for any variation of δ_∞ in the same range, ϕ_{shell} is higher and $C_{L^{z+}}^{shell}$ lower at 0.063 than at 0.25 g/L of lysozyme in the liquid.

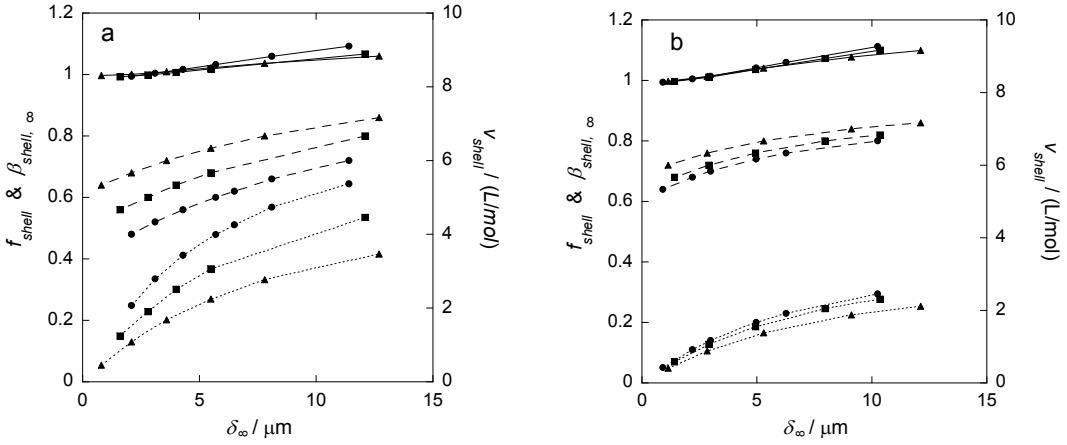

Figure S6.1. The variation of the model parameters f_{shell} (solid lines), $\beta_{shell,\infty}$ (dashed), and v_{shell} (dotted) with the final shell thickness δ_∞ used in the model fitting at (a) 40 mM and (b) 100 mM salt. Protein concentration in the liquid: 0.063 (triangles), 0.125 (squares), 0.25 g/L (dots).

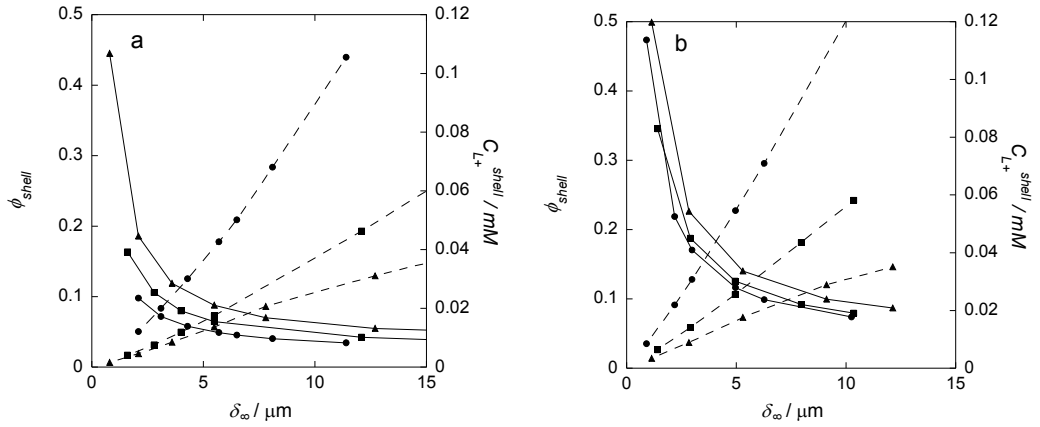

Figure S6.2. The variation of the model parameters ϕ_{shell} (solid lines) and $C^{shell}_{L^{z+}}$ (dashed) with the final shell thickness δ_∞ used in the model fitting at (a) 40 mM and (b) 100 mM salt. Protein concentration in the liquid: 0.063 (triangles), 0.125 (squares), 0.25 g/L (circles).

S7. Discussion of possible scenarios leading to an arrested shell structure

Initially the shell forms as protein molecules enter and collapse the network in the outer layers of the gel. As binding proceeds the position of the core/shell boundary (r_1) moves toward the centre of the gel. The continuous conversion of core to shell during this process is chiefly responsible for the deswelling of the gel. Due to the large difference in swelling between the shell and the core, the gel boundary (r_2) also moves closer to the centre, initially with nearly the same speed as the core/shell boundary. Thus, the progression of shell formation involves ordered motion of all molecules in the shell toward the gel centre, in response to elastic forces in the gel network. The motion is resisted by the viscous drag from water being "filtered" through the shell structure, and by the work of deforming the shell material. The latter arises in spherical geometry because the shrinking of the core forces volume elements in the shell to elongate radially and shorten laterally [6]. It is easy to see that the distance between two chains in the network of the shell, at the same distance from the

centre, will decrease with decreasing gel radius. At the same time, however, the distance between two chains at different distances to the centre increases. For constant density of the shells, as assumed here, and for the relative radial changes encountered in the experiments at 40 mM salt, a small initially cube-shaped volume element positioned in the shell close to the gel surface will at the end of deswelling assume an essentially rectangular parallelpiped shape. During the process, the shell network, which is initially in a highly anisotropic deformational state [7, 8], becomes more relaxed. Although it is difficult to draw any conclusions about how the deformation would affect the protein structure, three extreme scenarios leading to a finite shell thickness can be envisaged. Consider first shells in which the clusters already at an early point are connected both in the lateral and radial direction into a network. In scenario 1, the protein network continually rearranges during growth to maintain the same structure. However, the *time* required for rearrangements increases with the size of the structure (since it involves a larger number of molecules and rearrangements over larger distances) and at a certain shell thickness goes to infinity. The effect is thus kinetic, and the protein structure needs not be directly related to the deformational state of the polymer network in the shell. In scenario 2, the aggregate structure is deformed in a similar way as the polymer network. In this case the *work* of deforming the aggregate structure finally becomes too large. Here one can envisage an increased work of compressing the structure in the lateral direction, but also a work of extending it in the radial direction. Scenario 3 is similar to 2 but the clusters are initially of finite size and separated from each other in the shell. Here the concerted inward motion of the material in the shell (the freedom of the clusters to redistribute is limited due to the interaction with the polymer network) leads to an overlap of the clusters finally forming a percolated stress-bearing structure. Note, since the compression of a volume element in the lateral direction is compensated for by an extension in the radial

direction also scenario 2 and 3 can, in principle, can take place at constant protein volume fraction in the shell.

References for the Supporting Material

1. Göransson, A.; Hansson, P., *J. Phys. Chem. B* **2003,** 107, (35), 9203-9213.

2. Fan, L. T.; Singh, S. K., *Controlled Release. A Quantitative Treatment*. Springer-Verlag: Berlin, 1989; Vol. 13.

3. Coulson, J. M.; Richardson, J. F.; Blackhurst, J. R.; Harker, J. H., *Coulson & Richardson's Chemical Engineering*. 5 ed.; Butterworth-Heinemann: Oxford, 1996; Vol. 1.

4. Nilsson, P.; Hansson, P., *J. Phys. Chem. B* **2005,** 109, (50), 23843-56.

5. Johansson, C.; Hansson, P.; Malmsten, M., *J. Colloid Interface Sci.* **2007,** 316, (2), 350-359.

6. Nilsson, P.; Hansson, P., *J. Colloid Interface Sci.* **2008,** 325, (2), 316-323.

7. Hansson, P.; Schneider, S.; Lindman, B., *J. Phys. Chem. B* **2002,** 106, (38), 9777-9793.

8. Tomari, T.; Doi, M., *Macromolecules* **1995,** 28, (24), 8334-8343.